



African Journal of Biological Sciences



Bacillus Paralicheniformis: A potential candidate for natural antibacterial agents from marine macro-algae associated bacteria.

Sathyananth M¹, Ramkumar R²., Leon Stephan Raj T^{3*}., Shamal Kumbhar⁴., E. Jebarubi⁵., Virendra K Sangode⁶

¹Plant Molecular Biology Research Unit (PMRU), Department of Botany, St. Xavier's College, Palayamkottai, India (ORCID-<https://orcid.org/0000-0002-8972-0770>)

²Centre for Aquaculture Research & Extension, Department of Zoology, St. Xavier's College, Palayamkottai. <https://orcid.org/0009-0000-2238-4525>

³Director-PMRU, Assistant professor, Department of Botany, St. Xavier's College, Palayamkottai. (Affiliated to Manonmaniam Sundaranar. University. Abishekapatti) (ORCID ID: <https://orcid.org/0000-0001-6231-5962>)

⁴Department of Microbiology, Padamshree Vikhe Patil College of Arts, Science and Commerce, Pravaranagar, Loni, Tal-Rahata, Ahmednagar, Maharashtra, India <https://orcid.org/0009-0007-0563-4319>

⁵Plant Molecular Biology Research Unit (PMRU), Department of Botany, St. Xavier's College, Palayamkottai. India <https://orcid.org/0000-0003-3944-7179>

⁶Centre for Sericulture and Bioresource Management (CSBR) Assistant Professor M B Patel College of Arts Commerce And Science Affiliated to .RTM Nagpur University <https://orcid.org/0000-0002-4272-2744>

*Corresponding author—Leon Stephan Raj

*Email: leostephanraj@gmail.com

Article History

Volume 6, Issue 10, 2024

Received: 20 May 2024

Accepted: 15 June 2024

doi:

[10.48047/AFJBS.6.10.2024.6594-6618](https://doi.org/10.48047/AFJBS.6.10.2024.6594-6618)

ABSTRACT

Antibiotic resistance poses a major global health threat, necessitating new approaches to treat bacterial infections. We isolated bacteria from the brown macroalgae *Sargassum swartzii* collected along the Indian coast. Of 279 isolates, 47.6% showed antibacterial activity against *Staphylococcus aureus* and *Vibrio parahaemolyticus* when screened. Ten potent isolates underwent analysis of biosynthetic gene clusters and 16S rRNA sequencing. Isolate MP-99 carried polyketide synthase (pks) and non-ribosomal peptide synthetase (nrps) genes and exhibited antibacterial effects. 16S rRNA sequencing and species-specific markers confirmed the isolate MP-99 as *Bacillus paralicheniformis*. Gas chromatography-mass spectrometry revealed major components N-hydroxy methyl acetamide and dichloroacetic acid, 6-ethyl-3-octyl ester. The extract exhibited broad-spectrum antibacterial activity against *Klebsiella pneumoniae*, *Vibrio parahaemolyticus*, and methicillin-resistant *Staphylococcus aureus* (MRSA). It also potently inhibited biofilm formation by MRSA and *V. parahaemolyticus* at sub-microgram concentrations. Molecular docking suggested selective binding of certain isolate compounds to biofilm-associated proteins. The *B. paralicheniformis* extract showed moderate toxicity in an *Artemia salina* lethality assay. In conclusion, the marine isolate *Bacillus paralicheniformis* PMRU2.6 extract has promising antibacterial and antibiofilm potential against pathogens, warranting further research to develop safe therapeutic applications.

Keywords: Marine microbiome; *Bacillus paralicheniformis*; pks & nrps gene clusters; Antibacterial assay; Biofilm inhibition; Molecular docking; Toxicity.

INTRODUCTION:

Natural products from microbes are considered a promising component in the new era drug arsenal and are synthesized by certain traits localized in biosynthetic gene clusters (BGCs). Polyketide Synthases (PKS), Non-Ribosomal Peptide Synthetase (NRPS) are the largest natural Bio-product families widely synthesized by bacteria and fungi includes the antibiotics such as erythromycin (PKS) and vancomycin (NRPS). Around 24,000 natural PK and NRP products have been identified and characterized, including antibiotics and compounds with anti-tumor, immunosuppressant, anthelmintic and other biological activities [1,2]. Searching for PKS and NRPS genes can reveal an organism's biosynthesis potential. Screening these genes in marine macro algae-associated bacteria can detect new sequences and provide insight into the origin of macro algal components due to symbiosis.

Overuse of antibiotics has led to increased pathogen tolerance [3]. The marine biome is being extensively explored for novel antimicrobials, revealing untapped sources [4]. Marine microorganisms, including algae, fungi, and bacteria, generate bioactive metabolites utilized in bacterial infection treatments [5]. Symbiotically associated microorganisms are postulated to have enhanced bioactive secondary metabolite production [6]. It's suggested that secondary metabolites in marine ecosystems may be synthesized by symbiotic microorganisms. Their adaptability to diverse marine conditions may foster the development of novel bioactive compounds [7].

Biofilm is a microbial community with a distinct multicellular life cycle, in which cells undergo division and aggregation into clusters, microcolonies, and larger structures [8]. Biofilm can colonize any surface of higher eukaryotes, such as humans, and cause various diseases and infections [9]. Some examples of biofilm-associated infections in humans are dental caries, skin ulcers, and gastrointestinal disorders. Biofilm can also contaminate medical devices that are used in different clinical settings, and facilitate the transmission of pathogens through them [10]. Biofilm cells are encased in a matrix of extracellular polymeric substances (EPS), which is composed of polysaccharides, lipids, proteins, and extracellular DNA (eDNA) [11,12]. EPS provides biofilm cells with protection from environmental stressors and antimicrobial agents, and enhances their virulence and persistence in host tissues [13].

In response to the demand for an ample supply of innovative compounds exhibiting synergistic effects in the field of pharmacology, this particular study sought to explore the intricacies of the microbiome associated with Phaeophyceae member in an Indian coast of Gulf of Mannar, Tamilnadu, India which exhibits a high level of chemical interaction with the bacteria it coexists with. The results of this research have demonstrated the remarkable potential of the associated microbiome, revealing a promising candidate with significant antibacterial and bacterial biofilm inhibition. This research's significance lies in its potential to uncover novel bioactive compounds, expand our understanding of marine microbial diversity, contribute to sustainable drug discovery, and address the pressing issue of antibiotic resistance. It represents a promising advancement in biotechnological research and has important implications for human health and marine ecosystem conservation.

MATERIALS AND METHODS:**COLLECTION OF MARINE MACRO-ALGAE:**

Sargassum swartzii C. Agardh collected from five localities include west of the Gulf of Mannar,

India, from Mandabam (Ramanathapuram) to Muttom (Kanyakumari). The algal specimens were handpicked, washed, and sealed in a sterile zip lock covered with fresh marine water and shifted in an ice box to the laboratory.

ISOLATION OF ASSOCIATED BACTERIA:

The Algal tissue were washed thoroughly and homogenized with clean marine water aseptically to perform serial dilution up to 10^{-7} , and 100 μ l from 10^{-5} , 10^{-6} , and 10^{-7} dilution was inoculated in five replicates onto four isolation media with marine water of the sampling site: Soluble starch yeast extract peptone agar (SYP), Nutrient Agar (NA), Tryptone Soya Agar (TSA), and Zobell Marine agar 2216 without marine water (ZM) [14]. Each locality sample was plated on four media for each incubation type, with three replicates and three dilutions. One hundred eighty plates were incubated at 25°C in a BOD incubator. The plates were kept in a sterile transparent box lined with wet paper towels to prevent the drying of the media. The plates were incubated for up to 96 hrs. [15].

PURIFICATION OF ISOLATES:

Bacterial Colonies were selected morphologically, based on shape, form, surface elevation, edge, and pigmentation from the primary isolation media for 24 hrs intervals as described by Kaewkla and Franco [16], sub-streaked in ZMA plates and the isolated axenic colonies were stored on agar slants for short periods (4°C), and broth cultures were stored at -20°C with 20% sterile glycerol for future use. [17].

PRELIMINARY SCREENING OF MACRO ALGAE ASSOCIATED BACTERIA:

The preliminary screening of the isolates against Indicator strains *Staphylococcus aureus* (Gram-Positive) and *Vibrio parahaemolyticus* (Gram-Negative) was performed by agar well diffusion method [18]. Muller-Hinton agar (MHA - Himedia M173) plates were inoculated with indicator strain and approximately 6 mm well was made with a sterile gel puncture and loaded with 100 μ l of cell-free supernatant, and the plates were incubated at 30°C; 24h. Antibacterial activity was calculated by the Zone of inhibition (Zoi) in diameter (mm) [19].

SCREENING FOR BIOSYNTHETIC GENE CLUSTER (BGC)

Colony PCR technique was used for analyzing genome of the potential isolates. The pure colonies of isolates were directly infused into the 25 μ l of PCR Reaction mixture (GoTaq® Green Master Mix 1X - 12.5 μ l; Primers (0.5 μ M) Forward - 2 μ l and Reverse - 2 μ l; Nuclease-Free Water - 8.5 μ l). The PCR was done in T100 Gradient Thermal Cycler (Bio-Rad) with reaction conditions as initial denaturation at 95°C for 5 min, followed by 34 cycles of denaturation at 95 °C for 30 s, Annealing at 54°C - 56 °C for 30s and extension 72°C for 1.5 min. The final elongation at 68°C for 5 min and stored at 4°C. The PCR product of each potent isolates was purified by ExoSAP buffer (10:1) incubated 15 min at 37°C, followed by enzyme inactivation at 85°C for 5 minutes to remove the unwanted primers and dNTPs.

1. Polyketide synthase (pks-I and pks-II) were amplified using specific primers pks1-F (5' CGG GGC ACC GCC ATS AAC MAS GRC G 3') and pks1-R (5' CGC CCA GCG GGG TGS CSG TNC CGT G 3') for pks 1 gene [20]. pks-II was amplified using PF6 (5'TSGCSTGCTTGGAYGCSATC3') and PR6 (5'TGGAANCCGCCGAABCCGC T3') primers [21].

2. Adenylation (A) domain that encodes in NRPS gene clusters was amplified using A3F (5'GCSTACSYSATSTACACSTCSGG'3) and A7R (5'SASGTCVCCSG TSCGGTAS '3) primers [22].
3. The 16S rRNA gene was amplified in segments using the primer pairs 27F (5'GAGAGTTTGATCCTGGCTCAG3') and 1492R (5'TACGGTTACCTTGTT ACGACTT 3') [23], which produce a fragment of approx.-1500 bases.

PHYLOGENETIC STUDIES AND SPECIES IDENTIFICATION:

Automated Sanger di-deoxy chain termination sequencing was carried out using applied ABI 3500 DNA Analyzer (Applied Biosystems) at Rajiv Gandhi Centre for Biotechnology (RGCB) Thiruvananthapuram, Kerala, India. The PCR product of selected isolates pks and nrps derived nucleotide sequences were run in ORF Finder (<https://www.ncbi.nlm.nih.gov/orffinder/>) to translate the protein sequences (accessed on 22 May 2023). BLAST found the related proteins of deduced amino acid sequences against the Non-redundant (NR) Protein Database (BLASTP).

The 16S rRNA sequence obtained was compared against the genomic database using the nBLAST tool (<http://www.ncbi.nlm.nih.gov/BLAST>). Multiple sequence alignments were performed using the ClustalW tool and phylogenetic trees was constructed based on the neighbour-joining method using MEGA11 (v11.0.13) combined with bootstrap analysis using 1000 replications. The secondary structure of the coded sequence was predicted using RNAFold 2.4.

The pks and nrps Nucleotide gene sequences and 16S rRNA were submitted to the GenBank, NCBI, USA. Morphological and Biochemical characterization of potent isolates was studied according to Yadav et al. [24] and Verma et al. [25].

EXTRACTION OF BIOACTIVE COMPOUNDS FROM THE POTENT ISOLATE:

Culture condition Optimization: The growth parameters of the potent isolate were optimized for efficient carbon and nitrogen sources (0.5 – 2.0% w/v), % of NaCl, temperature, and pH. Zobell Marine Broth (ZMB) was modified with different carbon sources (glucose, lactose, starch, mannitol, xylose, and maltose) and nitrogen sources (peptone, ammonium sulfate, yeast extract, casein hydrolysate, soybean meal). The temperature ranged from 20 to 40°C and pH from 4 to 10. The parameters were tuned and the outcome was measured at OD- 600 nm using a spectrophotometer (Shimadzu, Japan).

The potent strain was cultured in optimal medium for 9 days at the optimized temperature on a rotary shaker at 110 rpm. Every 24 hours, 1 mL aliquots were collected, centrifuged, and the supernatant was concentrated to 0.05×10^3 mL using a vacuum evaporator. Antibacterial activity was assessed by measuring zones of inhibition.

The isolate was inoculated in 50 mL of optimized modified ZMB and incubated overnight at the optimum temperature until it reached the exponential phase. Then, 10 mL of the culture was transferred to a 7 x 1000 mL conical flask containing 7 x 700 mL of MB. The culture was incubated with constant shaking under the determined optimum conditions. After incubation, the culture was centrifuged at $6,000 \times g$ for 15 min at 4°C, and the supernatant was collected.

Extraction of Bio-active metabolites: A 10mL cell-free supernatant containing bioactive compounds was extracted using different solvents: n-Hexane (Hx), Ethyl acetate (EtOAc), Chloroform (CLF), and their mixtures: Hx&EtOAc (1:1), Hx& CLF (1:1), and Hx&EtOAc& CLF (1:1:1). The solvent profile with the best activity was selected. A total of 5L culture of the potent isolate was mixed with an equal volume of the selected solvent profile in a separating funnel. The immiscible upper layer was collected and concentrated using a rotary evaporator. Analysis was done using FTIR spectroscopy and Gas Chromatography-mass spectrometry (GC-MS). The

remaining extract was dried and stored at 4°C for further assays. Crude extracts dissolved in iso-octane were evaluated using a GCMS-QP2010 system (Shimadzu, Japan) as described by Pugazhendi et al. [26]. Volatile compounds were identified by comparing the retention time (Rt) and mass spectra (MS) with the NIST library search, considering a similarity index of < 92%. Acquired volatile compounds were analysed for its Pharmacokinetic Properties using the online tools SwissADME, AdmetSAR, and pkCSM.

DETERMINATION OF THE ANTIBACTERIAL ACTIVITY & MIC

The antimicrobial susceptibility of the bacterial broth extract was evaluated with the disc diffusion method as described previously by Carvalho et al. [27] against the selected indicator strains belongs to gram-positive bacteria (*Enterococcus faecalis* MTCC-439 & *MRSA* MTCC-) and gram-negative bacteria (*Pseudomonas aeruginosa* MTCC-1688; *Salmonella enterica* MTCC-3858; *Klebsiella pneumonia* MTCC-109 & *Vibrio parahaemolyticus* MTCC-451).

Overnight liquid cultures of indicator strains were centrifuged at 5,000 x g for 5 min at 10°C, and then suspended in PBS to 0.5 McFarland standard (1.0×10^6 CFU/mL; OD600). The indicator strain suspension was swabbed onto sterile MHA (HiMedia - M173). The extract was concentrated using a Rota E-Vap GREV 3 (India) then shade dried, and diluted with ethyl acetate to a known concentration of 50 µL. A 5mm disc was loaded with a 50 µL test sample (100, 50, 25, 12.5 mg) after inoculating the media. Streptomycin (10 mcg) and ethyl acetate served as positive (P) and negative (N) controls, respectively. Three replicates were performed for each concentration. The cultures were incubated in a BOD incubator (Technico, India) at 27 ± 2 °C for 24 hrs, and the zone of inhibition in diameter was evaluated. The relative percentage inhibitions (PIs) for the ethyl acetate extract compared to the positive control were calculated by following formula,

$$PI = \frac{100 \times (X - Y)}{(Z - Y)}$$

Where X = Mean test extract, Y = Mean negative control, Z = Mean positive control.

The minimum inhibitory concentration of the extract was found against by broth microtiter dilution method using Tetrazolium salt [28,29,30]. Initial concentrations were reduced to half on the next well from 128 to 0.25 µg, and further inter dilutions were pathogen-specific. Color change from yellow (Tetrazolium) to purple (Formazan) showed the presence of live cells in the well. The MIC concentration was expressed in µg/ mL.

DETERMINATION OF ANTI-BIOFILM ACTIVITY:

Anti-biofilm activity of the potent isolate was detected and visualized using Crystal violet staining method reported by Liu et al. [31]. In Brief, overnight cultured *MRSA* and *V. parahaemolyticus* was diluted with fresh Tryptic soya broth to a final concentration of $\sim 1 \times 10^6$ CFU/ mL and culture under static condition to attain preformed microbial biofilm. A known volume of extract was added to culture tubes, with two control tubes for each biofilm-forming bacterium. After 24-hour incubation at 37°C, the liquid media was removed, leaving the biofilm intact. The biofilm was stained with 0.50% crystal violet for 10 min, washed with PBS, and de-stained with 100 µL of ethanol. The absorbance at 570 nm was detected with a UV spectrophotometer to quantify the biofilm biomass and the following equation was used to find

$$\text{Biofilm inhibition (\%)} = \frac{\text{Control OD 570 nm} - \text{Test OD 570 nm}}{\text{Control OD 570 nm}} \times 100$$

Molecular docking analysis: The key components of the potent isolate's extract were virtually analyzed using the docking procedure in Autodock vina in PyRx with protein and ligand preparation and visualized in Discovery studio. 7C7U an Biofilm associated protein – BSP domain and 6MLT Biofilm matrix protein Bap1 were used as target protein.

TOXICITY ASSAY:

Brine Shrimp Lethality Bioassay was used to determine the toxicity of the bacterial extracts upon the crustacean amphipod *Artemia salina* [32]. Briefly, *Artemia salina* larvae of similar age were transfer in a test vial, each containing 10 mL of saltwater (30ppt) with different concentrations of bacterial extract, and incubated at 27°C for 24 hrs under light. After incubation, a sample of the vial was taken and the surviving larvae were counted. Each sample was analyzed in triplicate, and the mean value was recorded. The death rate of each concentration was determined by using the formula;

$$\text{Mortality \%} = 100 \times \frac{\text{Number of dead nauplii}}{\text{Number of dead nauplii} + \text{Number of live nauplii}}$$

The lethal concentration (LC50) value was determined by converting the percentage of mortality to the probit value. The LC50 was determined using the fit line by linear regression analysis according to Meyer et al. [33]. Impact of extract on Morphological *A. salina* was analyzed by the exposure of extract with the *A. salina* for 1 hr.MP then observed under microscope.

STATISTICAL ANALYSIS

Statistical analysis of the all the above data was performed using SPSS version 22.0 (Statistical package deal for the Social Sciences, Inc., Chicago, U.S.A.). All results were compared with an Analysis of Variance (ANOVA) observed through a Bonferroni hoc evaluation. Outcomes were taken into consideration as statistically significant at p-value < 0.05.

RESULT:

ISOLATION OF MARINE ALGAE ASSOCIATED BACTERIA:

The five localities were tagged as MD (Mandabam), HI (Hare Island), MP (Manapaadu), IK (Idinthakarai), and MM (Muttom). Two hundred seventy-nine colonies were isolated from the *Sargassum swartzii* C. Agardh based on colonial morphology, and the pure strains were named MD-01 to MD-56; HI-57 to HI-77; MP-78 to MP-156; IK-157 to IK-214 and MM- 215 to MM-279. These strains were cultured and maintained in Zobell marine Agar. **PRELIMINARY SCREENING OF**

MACRO ALGAE ASSOCIATED BACTERIA:

Bacterial isolates were screened against human pathogen's indicator strain. Only 133 (47.6%) showed positive activity and the remaining 42.4% showed a negative effect against the indicator strains. The percentage of activity against *Staphylococcus aureus* (MTCC-96) is 28.4% and *V. parahaemolyticus* (MTCC-451) is 19.2% (Figure S1:A& B). Among them, MD-12, MD-28, HI-61, HI-62, MP-99, MP-123, IK-211, IK-214, MM-230 and MM-277 wereshowed relatively high activity (> 5mm – radius) have underwent pks and nrps Gene screening and 16SrRNA sequencing studies. (Table:1)

SCREENING FOR BIOSYNTHETIC GENE CLUSTER (BGC)

Ten potent isolates were screened for pks1, pks2, and nrps genes using PCR with specific primers. Isolate IK-211 exhibited positive results for all three genes. Isolates HI-62 and IK-214 did not

show significant gene presence. Preliminary antibacterial activity, 16S rRNA sequence homology, and gene presence data were tabulated in Table:1.

Isolate MP-99, displaying inhibition in the preliminary assay and carrying pks1 and nrps genes, was selected for further analysis. BLAST analysis revealed the highest similarity of MP-99's pks1 gene with type I polyketide synthase (WP143261071.1) and its nrps gene with Non-Ribosomal Peptide Synthetase (WP122934926.1) from *Bacillus paralicheniformis*. The sequences were deposited in the NCBI database with accession numbers OQ128064 and OQ128065 for pks1 and nrps genes, respectively. Additionally, the nucleotide sequences of pks and nrps were translated and subjected to phylogenetic analysis (Figure S2 & S3) using ORF finder and BLAST against the Non-redundant protein sequence (nr) database.

| Test Strain | Preliminary Assay (Zol) | 16S rRNA Gene Homology (%) with Type Strains | Presence of PKS gene cluster (pks1 & pks2) | Presence of NRPS gene cluster (nrps) |
|--|-------------------------|---|--|--------------------------------------|
| MD-12 | ++ | <i>Vibrio harveyi</i> (KU197879.1) 99.60% | - | nrps |
| MD-28 | +++ | <i>Photobacterium rosenbergii</i> (MN339950.1) 99.74% | - | nrps |
| HI-61 | ++ | <i>Bacillus velezensis</i> (CP054714.1) 100% | pks1 | - |
| HI-62 | + | <i>Aeromonas veronii</i> (MT345040.1) 99.10% | - | - |
| MP-99 | +++ | <i>Bacillus paralicheniformis</i> (MK332356.1) 100% | pks1 | nrps |
| MP-123 | + | <i>Pseudoalteromonas piscicida</i> (NR_114583.1) 99.72% | pks1 | - |
| IK-211 | + | <i>Pseudomonas fluorescens</i> (MT775496.1) 99.86% | pks1 & pks2 | nrps |
| IK-214 | +++ | <i>Vibrio sp</i> (ON139202.1) 100% | - | - |
| MM-230 | ++ | <i>Escherichia coli</i> (CP097721.1) 99.92% | pks2 | - |
| MM-277 | + | <i>Vibrio sp</i> (AB571869.1) 100% | - | nrps |
| <5mm = '+'; 5 to 10 mm = '++'; >10mm = '+++' | | | | |

16S rRNA SEQUENCING:

The potent strain MP-99 was sequenced, revealing a 1374 bp 16S rRNA coding region. A BLAST comparison against the NCBI database showed 100% query cover and 99.16% identity with *Bacillus paralicheniformis* (MK332356.1). Phylogenetic analysis using MEGA11 software confirmed its evolutionary relationship with the 16S rRNA sequence of the *Bacillus paralicheniformis* strain KJ-16 (Figure 1). *Bacillus mycoides* served as an outgroup in the analysis. The genetic distance matrix suggests that MP-99 is a strain within the *B. paralicheniformis* species, being closely related to

strains KJ-16, slightly more distant from *Bacillus licheniformis* strain DSM, and more divergent from *Bacillus mycoides* strain DSM 11821.

The 16S rRNA sequence displayed an optimal secondary structure (Figure S4) with a Minimum Free Energy (MFE) of -517.90 kcal/mol. The free energy of the thermodynamic ensemble was -537.35 kcal/mol, with a diversity of 225.93 units and a 0.00% frequency of MFE in dot-bracket notation. The structure was color-coded based on base-pairing probabilities, while unpaired regions were denoted by color indicating the likelihood of being unpaired.

SPECIES – SPECIFIC AMPLICONS FOR IDENTIFICATION:

The isolated active strain *Bacillus paralicheniformis* PMRU2.6 have maximum similarity with the whole genome of *Bacillus paralicheniformis* (JARZfZ010000002.1) have chosen for antiSMASH (<https://antismash.secondarymetabolites.org/>) analysis and found the Fengycin biosynthetic gene cluster from *Bacillus velezensis* FZB42 (MIBiG accession: BGC0001095) in its genome (Location: 3,257,360 – 3,335,026 nt. (total: 77,667 nt)) with 86% of identity. Fengycin coding *fenC* and *fenD* domain were amplified using the primers early reported by Olajide et al. [34] where the annealing temperature was shifted to 54°C and amplicons *fenD* were found to have 900 bp band and no band formed in *fenC* primers in the genome (Figure 2). *Bacillus subtilis* (MTCC 121) was served as control.

Based on phylogenetic analysis and Fengycin based markers identification the isolate MP-99 was designated as *Bacillus paralicheniformis* PMRU2.6. sequence was submitted to the gene bank (NCBI) and assigned the Acc. No: OP393887.1. This is a gram-positive, motile, rod-shaped bacteria tested positive for catalase, starch, nitrate reduction, Gelatinase, Mannitol fermentation, and sorbitol fermentation.

EXTRACTION OF BIOACTIVE COMPOUNDS FROM THE POTENT ISOLATE

Culture Condition Optimization: Different broths are used to assess the best for Antibacterial Compound Production. Modified Zobell Marine broth with Maltose (1.2% w/v) and Ammonium sulfate (0.8% w/v) with NaCl concentration of 8% w/v had comparably greater effect than other C and N sources. The optimum condition for the potent strain's secondary metabolite production was $32 \pm 0.8^\circ\text{C}$ for 96 hrs with pH 7.2 ± 1 . Solvent for Extraction: Cell-free supernatant of the cultured potent isolate in a optimized condition was extracted with different solvents were tested against MRSA and *V. parahaemolyticus* using a Disc Diffusion assay, Ethyl acetate showed the greater inhibition, followed by EtOAc: CLF, Hx: EtOAc, and other solvents. Hence, Ethyl acetate was used for extraction and further studies.

Analysis of Extract: GC-MS analysis had produced 18 peaks on Ethyl acetate extract which were confirmed by FT-IR functional group analysis (Figure: 3; Table: 2). As shown in the Figure 4, the major constituents in ethyl acetate crude extract of MP-99 were identified at retention time 3.018 min as N-hydroxy methyl acetamide, which has a molecular weight of 89.09 g/mol and a molecular formula of $\text{C}_3\text{H}_7\text{NO}_2$. Following this, there was Dichloroacetic acid, 6-ethyl-3-octyl ester at 10.837 min with a molecular weight of 269.20 g/mol and a molecular formula of $\text{C}_{12}\text{H}_{22}\text{Cl}_2\text{O}_2$. This confirms the presence of these two compounds in the crude extract of MP-99. The mass spectrum of Dichloroacetic acid, 6-ethyl-3-octyl ester and N-Hydroxy-N-methyl acetamide along with Insilco analysis (Swiss target prediction and physiochemical space for oral availability) was charted in Figure S5- A & B. Pharmacokinetics analysis on Dichloroacetic acid, 6-ethyl-3-octyl ester and N-Hydroxy-N-methylacetamide adhered to drug-like compounds with high oral bioavailability and blood-brain barrier penetration, but different CYP2C9 inhibition and Veber's rule compliance (Table:3).

Table: 2 GC-MS and FTIR analysis of crude extract showing Antibacterial activity that has previously reported.

| GC-MS | | | | | FT-IR | | |
|--------|--|--------------|-------------|--------|--------------------|-------|-------------------|
| RT | Compound name | Mol. Formula | Mol. Weight | Area % | Wave Number (cm-1) | %T | Functional groups |
| 3.018 | N-hydroxymethyl acetamide | C3H7NO2 | 89.09 | 18.688 | 1246.23 | 04.98 | Amine |
| 10.716 | 1-hexanol, 5-methyl- 2-(1-methylethyl) | C10H22O | 158.28 | 7.204 | 1058.91 | 10.99 | Primary alcohol |
| 10.837 | Dichloroacetic acid, 6-ethyl-3-octyl ester | C12H22Cl2O2 | 269.20 | 11.305 | - | - | Ester/chloro |
| 10.952 | 1-octanol, 2-butyl | C12H26O | 186.33 | 8.415 | 1058.91 | 10.99 | Primary alcohol |
| 12.867 | Ether, hexyl pentyl | C11H24O | 172.31 | 2.499 | 1111.15 | 11.20 | Aliphatic ether |
| 16.249 | 1-Tridecanol | C13H28O | 200.36 | 6.438 | 1058.91 | 10.99 | Primary alcohol |
| 22.186 | 9-octadecenamide | C18H35ON | 128.13 | 7.542 | 1246.23 | 04.98 | Amine |

Table:3 Pharmacokinetics analysis of Dichloroacetic acid, 6-ethyl-3-octyl ester and N-Hydroxy-N-methylacetamide

| Property | Dichloroacetic acid- | N-Hydroxy-N methylacetamide |
|-------------------------|----------------------|-----------------------------|
| GI absorption | High | High |
| BBB permeation | + | + |
| P-gp substrate | - | - |
| CYP2C9 inhibition | + | - |
| Lipinski's rule | Pass | Pass |
| Ghose filter | Pass | Pass |
| Veber's rule | Pass | Fail (1 violation) |
| Bio-availability score | 0.55 | 0.55 |
| PAINS alerts | 0 | 0 |
| Synthetic accessibility | 3.04 | 2.07 |

GI - Gut Intestinal; BBB - Blood-brain barrier; P-gp - P-glycoprotein; CYP2C9 - Cytochrome P450 enzyme; PAINS - pan-assay interference compounds.

--

DETERMINATION OF ANTIBACTERIAL ACTIVITY & MIC

The EtOAc extract of strain MP-99 exhibited variable inhibitory activity against tested pathogenic bacteria. The tested indicator strains displayed specific inhibition by the extracted metabolite from

the potent isolate *Bacillus paralicheniformis* PMRU2.6 demonstrated antibacterial activity in Tables:4 (Figure S6). A significant reduction in *K. pneumonia* growth ($77.89 \pm 0.76\%$ inhibition) was observed with 100mg of EtOAc extract ($df = 5, 1; F = 4.132; p < 0.001$). The extract also showed notable inhibition against *V. parahaemolyticus* ($75.61 \pm 1.24\%$) and MRSA ($64.9 \pm 1.63\%$). Further analysis is needed before utilizing this material for infectious pathogens management. Significantly different correlations were found between 100mg and 12.5mg ($p < 0.001$), 100mg and 25mg ($p < 0.002$), 100mg and 50mg ($p < 0.001$), and other lower concentrations except 12.5 mg and 25mg ($p < 0.2$). These correlations were statistically significant at the 0.01 level, indicating a strong relationship between the variables. (Table:5).

MIC: The MIC of the extract lies between 54 - 76 $\mu\text{g}/\text{mL}$ was confirmed with its independent triplicate data and noted as Mean \pm SD in (Table:4). The stability of the Cell-free supernatant with bioactive metabolite at different temperatures, pH, and duration was evaluated and confirmed to retain its inhibitory ability with a range of factors studied. (Temp= - 20° - 100°C; pH = 2 to 10; storage- Stable without loss of function)

| Table:4 Impact of <i>B. paralicheniformis</i> extract on antibacterial activity and its MIC | | | |
|---|-------------------------------|-------------------------|---------------------------------|
| Pathogen | EtOAc MP-99 (μg) | Zone of inhibition (mm) | MIC ($\mu\text{g}/\text{mL}$) |
| Klebsiella pneumonia | 12.5 | 8.2 ± 0.2 a | 77.89 ± 0.7 |
| | 25 | 13 ± 0.2 b | |
| | 50 | 18.5 ± 0.2 c | |
| | 100 | 21.5 ± 0.2 d | |
| | Streptomycin | 26.5 ± 0.2 a | |
| | Ethyl acetate | 2.2 ± 0.1 e | |
| Salmonella enterica | 12.5 | 7.2 ± 0.6 a | 74.3 ± 0.6 |
| | 25 | 9.6 ± 0.3 b | |
| | 50 | 12.7 ± 0.1 c | |
| | 100 | 16.6 ± 0.3 d | |
| | Streptomycin | 20.5 ± 0.2 d | |
| | Ethyl acetate | 1.3 ± 0.1 e | |
| Vibrio parahaemolyticus | 12.5 | 8.5 ± 0.2 a | 75.61 ± 1.2 |
| | 25 | 10.5 ± 0.2 c | |
| | 50 | 15.5 ± 0.2 c | |
| | 100 | 20 ± 0.4 d | |
| | Streptomycin | 25.7 ± 0.1 a | |
| | Ethyl acetate | 2.2 ± 0.2 e | |
| MRSA | 12.5 | 11.2 ± 0.2 b | 64.9 ± 1.6 |
| | 25 | 15.3 ± 0.3 c | |
| | 50 | 18.5 ± 0.2 c | |
| | 100 | 21.7 ± 0.3 d | |
| | Streptomycin | 30.3 ± 0.2 a | |
| | Ethyl acetate | 3.5 ± 0.2 e | |
| Enterococcus faecalis | 12.5 | 10.3 ± 0.2 a | 54.2 ± 0.6 |
| | 25 | 15 ± 0.2 c | |
| | 50 | 19 ± 0.2 c | |
| | 100 | 22 ± 0.3 d | |

| | |
|---------------|--------------|
| Streptomycin | 29.3 ± 0.6 a |
| Ethyl acetate | 3.1 ± 0.1 e |

Data represent Mean ± SD of triplicates independent experiments.
Streptomycin – Positive control (30 µg). Ethyl acetate – Negative control.

Table:5 Impact of EtOAc extract concentrations on inhibition of indicator strains

| Extract conc. (µg) | Statistics | Percentage of Inhibition | | | | | Dosage Statistics | | |
|--------------------|------------------|--------------------------|------------------|---------------------|--------------|--------------|-------------------|--------------|-------|
| | | K. pneumonia | S. enterica | V. parahaemolyticus | MRSA | E. faecalis | t | F | p |
| | | 12.5 | $\bar{x} \pm SE$ | 22.8 ± 1.17 | 29.74 ± 1.12 | 27.9 ± 0.85 | 29.78 ± 0.64 | 26.64 ± 0.58 | 4.595 |
| 25 | $\bar{x} \pm SE$ | 41.41 ± 1.47 | 41.18 ± 1.06 | 37.37 ± 1.27 | 44.5 ± 1.25 | 45.58 ± 1.25 | 1.529 | 2.337 | .032 |
| 50 | $\bar{x} \pm SE$ | 67.74 ± 1.05 | 61.78 ± 1.37 | 58.46 ± 1.16 | 54.94 ± 1.23 | 64.65 ± 2.43 | 1.813 | 3.286 | .05 |
| 100 | $\bar{x} \pm SE$ | 77.89 ± 0.76 | 77.76 ± 1.23 | 75.61 ± 1.24 | 64.9 ± 1.63 | 75.77 ± 2.12 | 1.931 | 3.729 | .049 |
| ANOV A | df | 5,1 | 5,1 | 5,1 | 5,1 | 5,1 | - | - | - |
| | F | 4.132 | 3.639 | 2.966 | 1.662 | 2.422 | - | - | - |
| | p | .001 | .002 | .009 | .041 | .013 | - | - | - |

Determination of Anti-Biofilm Activity:

Biofilm on the host by the pathogenic bacteria is a common initiative factors in enhancing antibiotic-resistance in bacteria. The biofilm inhibitory potential of the MP99 metabolites was investigated. The results (Figure:5) suggested that the isolates had the potential to inhibit the preformed biofilm of V. parahaemolyticus and MRSA up to 94.39 % and 95.56% respectively could be achieved at significantly lower concentration of the metabolites; The minimal concentration for biofilm inhibition (BIC) was found as IC50 =25.430 µg/ml, IC90 = 65.369 µg/ml for V. parahaemolyticus (t = 12.768) where 1.82% was a Standard error from the total Mean value and for MRSA IC50 = 30.116 µg/ml. IC90 = 63.193 µg/ml (t = 9.797) where 3.56 % was a Standard error. (p > 0.001).

Molecular docking analysis revealed differential binding of isolate metabolites to the two biofilm-associated protein targets 7C7U and 6MLT was Tabulated in Table: 6; Figure S7). The top binding compounds against 7C7U were 1-octanol 2-butyl with a docking score of -5.2 kcal/mol and 1-hexanol derivative at -5.1 kcal/mol. Against 6MLT, 1-hexanol derivative exhibited the strongest affinity at -4.5 kcal/mol, followed by 1-octanol 2-butyl at -4.3 kcal/mol. These results highlight the ability of certain isolate compounds to preferentially bind to biofilm proteins involved in cell aggregation (7C7U) versus matrix stability (6MLT). The selective hitscan serve as starting points for structure-based lead optimization efforts to improve potency and selectivity for each target.

Table:6 Molecular docking Binding affinity (kcal/mol)

| Ligands | 7C7U | 6MLT |
|---------------------------------------|------|------|
| 9-octadecenamide | -4.5 | -4.7 |
| 1-octanol, 2-butyl | -5.2 | -4.3 |
| Ether, hexyl pentyl | -4.6 | -4 |
| 1-Tridecanol | -4.2 | -4 |
| 1-hexanol, 5-methyl-2-(1-methylethyl) | -5.1 | -4.9 |
| N-hydroxymethyl acetamide | -4.3 | -3.8 |

TOXICITY ASSAY:

The in-vivo cytotoxicity of the ethyl acetate extract of MP-99 was determined by brine shrimp lethality bioassay. LC50 values were estimated from the plot of mortality percentage versus the log of sample concentrations (Table:7; Figure S8). The LC50 of the extract was 132.84 µg/mL (95% confidence limits: 94.83 – 187.73). Under similar conditions, vincristine, the positive control, displayed an LC50 of 1.92 ± 0.23 µg/mL, indicating its significantly higher toxicity based on both toxicity indices. Pearson's Goodness-of-Fit Test revealed a statistically significant Chi-Square value of 18.040 (df = 19, p = 0.016) at the 5% level. Morphological observations at 100 ppm showed minimal negative effects. Though some loss of motility was seen, thoracopods, antennae, and gonads remained intact without rupturing. However, loss of contraction occurred in rectum and telson tissues of all treated animals. In contrast, at maximum dosage complete degradation was observed by the 24th hour. (Figure S9).

Table: 4 Brine shrimp response to the Extract

| Conc. (ppm) | Brine shrimp response | | 95% Confidence Limits | |
|-------------|-----------------------|---------------|----------------------------|--------------------------------|
| | Mean ± SE | Mortality (%) | LC50 | LC90 |
| 5 | 0.3 ± 0.3 a | 3.3 ± 3.3 | 132.84 (94.83 – 187.73) | 1025.569 (621.91 – 2147.27) |
| 10 | 1.3 ± 0.3 a | 13.3 ± 3.3 | | |
| 50 | 1.6 ± 0.3 a | 16.6 ± 3.3 | | |
| 100 | 3.6 ± 0.3 b | 36.6 ± 3.3 | | |
| 250 | 5.3 ± 0.3 c | 53.3 ± 3.3 | | |
| 500 | 8.3 ± 0.3 d | 83.3 ± 3.3 | | |
| 1000 | 10 ± 0.0 e | 100 ± 0 | | |

ANOVA: df = 6, 1; F= 142.889; p= <. 0001

DISCUSSION:

Evolutionary evidence suggests that marine bacteria and algae emerged from shared prokaryotic ancestors. Marine bacteria excel at bioremediating toxic pollutants like heavy metals, hydrocarbons, and xenobiotics through specialized extracellular secretions and biofilm formation [35]. These extracellular polymeric substances (EPS) enable aggregation and protection from

environmental stressors. Such interdependencies between bacteria and algae exemplify the enriching ecological relationships that define marine microbial niches [36,37]. These intricate interactions, spanning coevolution to metabolite production, offer insights from microbial ecology to drug discovery. Previous studies have elucidated specific synergistic associations between bacteria and algae, highlighting the biodiversity underpinning their shared marine habitats.

Our current investigation focused on the bacterial communities associated with specific brown macro-algae using low-nutrient primary isolation media. Similar studies from Brazil using a sponge sample yielded fewer than 158 colony-forming units (CFU) [38]. In our study, 47% of the total isolates displayed positive activity against the selected pathogens, *Staphylococcus aureus* and *Vibrio parahaemolyticus*. Ten isolates with the highest inhibitory action were chosen for further screening of the pks and nrps genes in *Bacillus paralicheniformis*. *Bacillus* sp. from marine ecosystems have previously been reported to produce Bogorol (*Bacillus laterosporus*), leodoglucomide C, and leodoglycolipid (*Bacilluslicheniformis*) [39], all of which exhibit high potential against bacterial and fungal pathogens. This suggests that these isolates with closer phylogenetic relationships have a greater possibility of sharing antagonistic traits.

The marine environment harbors diverse macro- and microorganisms that have evolved specific metabolic capabilities to ensure survival in hostile environments. This results in unique secondary metabolites with commercial value for pharmaceutical and cosmetic industries [40]. Ethyl acetate was found to be the most effective solvent for extracting antimicrobial compounds from several *Bacillus* sp., consistent with previous findings [41, 42].

Bacillus species produce several high-molecular-weight lipopeptides (>1000 daltons) with antibacterial and antifungal properties. While most are encoded by nrps biosynthetic gene clusters (BGCs), the Iturin family is encoded by a hybrid PKS-I/NRPS system [43]. However, even close phylogenetic relatives with nearly identical 16S rRNA gene sequences (99.4% similarity) can show limited sharing of pks and nrps gene clusters and other species-specific secondary metabolite biosynthetic pathways [44,45].

Fengycin, a reported lipopeptide in *Bacillus* sp., exhibits enhanced inhibitory activity against bacteria and fungi [46,47]. Species-specific markers (fenC and fenD) have been used to distinguish *B. paralicheniformis* from its close relative *B. licheniformis* [34]. Our isolate formed a distinct band on fenD amplicons around 900 bp, exceeding the 700 bp amplicon length reported by Olajide et al. [34]. While fenC amplification proved unsuccessful, potentially hindering definitive species identification based solely on this marker, the combined evidence from phylogenomic analysis of the 16S rRNA sequence and the distinctive fenD amplicon size strongly supports the isolate's classification as *B. paralicheniformis*.

The cyclic polypeptide Bacitracin was previously reported in *B. licheniformis* and *B. subtilis* [48,49]. PCR analysis using primers based on *B. licheniformis* bacitracin synthetase gene detected a matching sequence in our isolate (*B. paralicheniformis* PMRU2.6), suggesting conservation within *Bacillus*.

Dichloroacetic acid, 6-ethyl-3-octyl ester possesses anticancer activity [50] and favorable physicochemical properties for oral bioavailability and enzyme/receptor binding. It may primarily target the estrogen receptor beta.

Iqbal et al. [51] reported *B. paralicheniformis* ES-1 inhibited *S. aureus* up to 35%. In contrast, our study shows significantly higher activity against MRSA (65%) and other pathogens (exceeding 75%). Inhibition of *V. parahaemolyticus* suggests growth promotion by controlling vibriosis in shellfish. *Bacillus* antimicrobial peptides align with related probiotics' beneficial properties for aquatic farms [52]. MRSA's unique genetic makeup and methicillin resistance pose a challenge. Metabolite

extracts from MP-99 have potent antibiofilm activity against MRSA and *V. parahaemolyticus*. Biofilm formation by MRSA can contribute to several infections, including skin and soft tissue infections, urinary tract infections, bone and joint infections, bacteremia, infective endocarditis, respiratory tract infections, and central nervous system and eye infections [53]. Similarly, the pathogen *V. parahaemolyticus* can cause gastroenteritis, wound infections, and septicemia. Biofilm formation enhances its resistance and persistence, resulting in difficult-to-treat infections [54]. Quorum sensing and virulence regulators influence *V. parahaemolyticus* biofilm formation by modulating the secretion of toxins, adhesion molecules, and other factors [55,56]. Within biofilms, bacteria become more resistant to antibiotics and better able to evade the immune system [57]. Biofilm-associated phenotypes thus contribute to the pathogenicity and recalcitrance of *V. parahaemolyticus*.

Current study reveals that at concentrations below 100 µg/ml, the metabolites inhibited over 90% of biofilm formation, with IC50 values of 25 and 30 µg/ml against *V. parahaemolyticus* and MRSA, respectively. This broad efficacy against both Gram-positive and Gram-negative biofilm formers demonstrates the promising therapeutic potential of isolate MP-99 metabolites, similar and efficient than the antibiofilm activity early reported against *B. pumilus* and *B. indicus* extracts against *Pseudomonas aeruginosa*. [58]

Molecular docking simulations provided valuable insights into the binding interactions between the MP-99 metabolites and biofilm-associated proteins. Interestingly, the differential binding energy profiles revealed that certain compounds displayed selective affinity for the cell aggregation mediator 7C7U compared to the matrix protein 6MLT. This observation aligns with findings by Khidre et al. [59]. Such selectively binding compounds hold immense promise as starting points for structure-based design of inhibitors against crucial virulence factors like 7C7U, which play pivotal roles in bacterial pathogenesis [60]. Harnessing these diverse compounds presents an attractive anti-virulence strategy to combat the biofilm-associated recalcitrance and pathogenicity of bacteria like *V. parahaemolyticus* and MRSA.

The MP-99 extract exhibits a dual toxicity profile according to Meyer's [33] and Clarkson's [61] indices. It demonstrates potent activity with an LC50 below 1000 µg/mL, warranting further scrutiny. Concurrently, it displays moderate toxicity with an LC50 between 100 and 500 µg/mL, indicating a complex behavior. Morphological examinations revealed no organ deformities, and the observed digestive tract effects align with typical side effects of novel dietary additives.

The MP-99 extract displayed both toxic and moderately toxic activities, revealing potential for diverse biological interactions. Further exploration to identify specific targets is crucial to harness these interactions positively. This assessment of the marine microbiome's bioactivity provides a new perspective, showcasing the complex and intriguing potential of the *Bacillus paralicheniformis* extract. Elucidating precise mechanisms and targeted effects could enable non-harmful applications, unlocking novel beneficial uses in various biological contexts.

CONCLUSION:

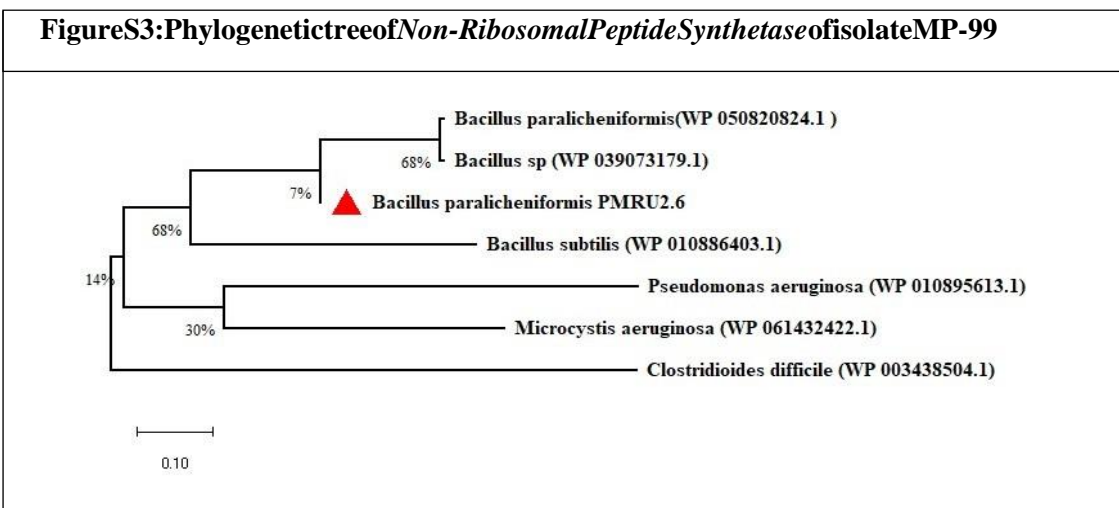
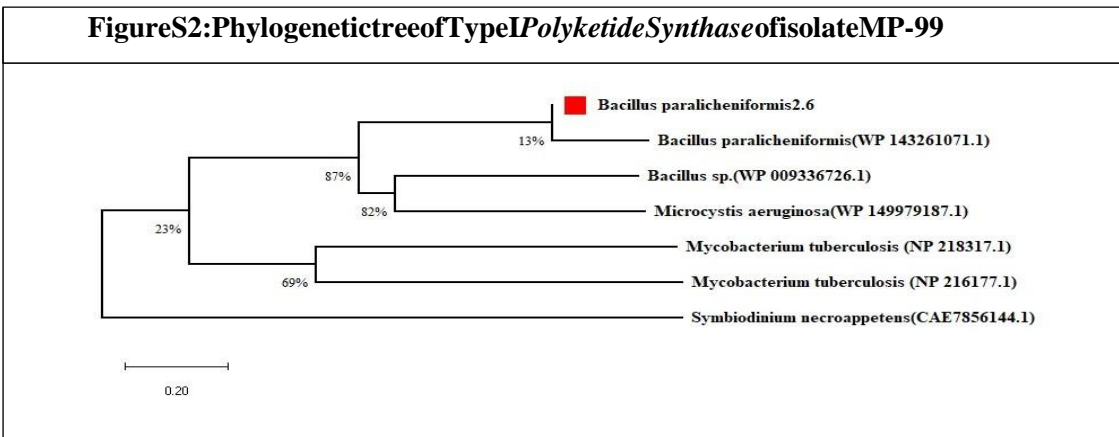
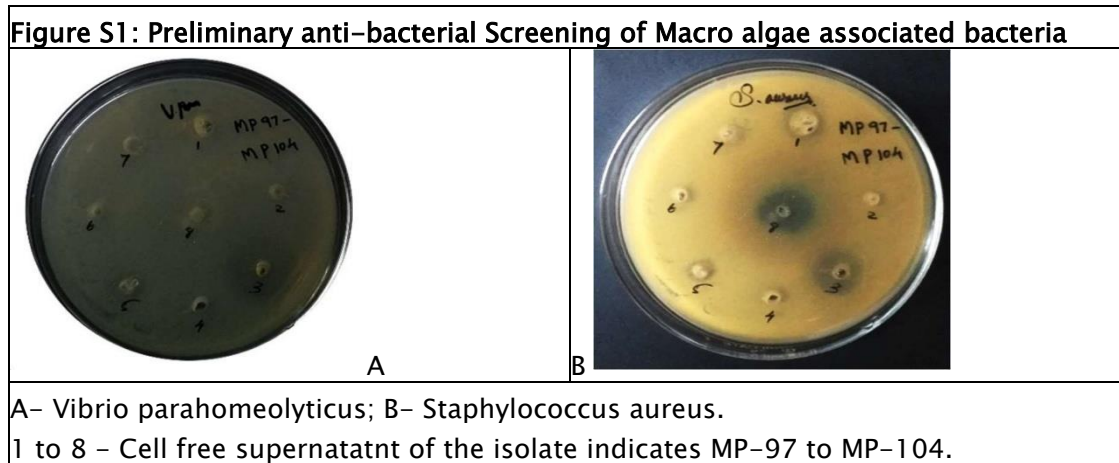
This study revealed the promising antibacterial and antibiofilm potential of the marine isolate *Bacillus paralicheniformis* PMRU2.6. Its ethyl acetate extract exhibited broad-spectrum activity against pathogens including MRSA and strongly inhibited Gram-positive and Gram-negative biofilm formation. Molecular docking suggested selective targeting of biofilm proteins, indicating an anti-virulence mechanism. While moderately toxic to brine shrimp, further research on specific biological targets may enable safe and beneficial applications. This highlights the value of marine bacteria like PMRU2.6 for developing new therapies against drug-resistant and biofilm infections.

Competing Interests:

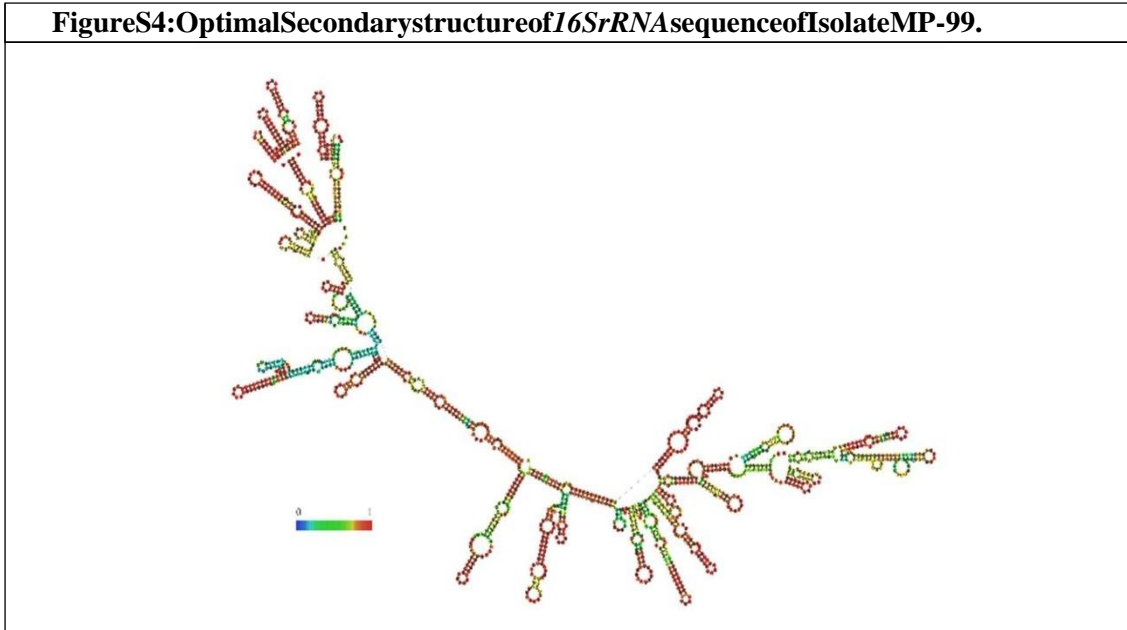
The authors declare no competing financial interest.

Contributions:

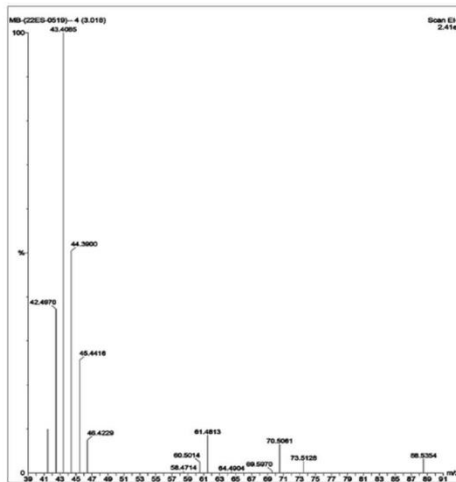
All authors contributed to the study conception and design. Sampling and data collection and analysis were performed by all the authors. The first draft of the manuscript was written by Sathyananth M and all authors commented on previous versions of the manuscript. All authors read and approved the final manuscript.



FigureS4:OptimalSecondarystructureof16SrRNAsequenceofIsolateMP-99.

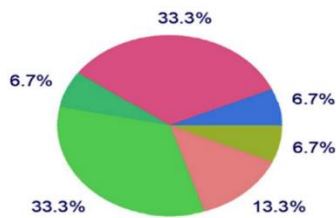
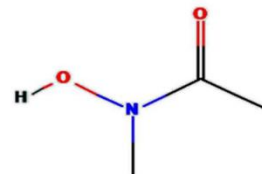


B



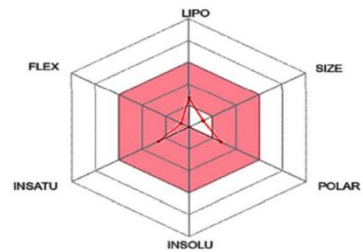
N-Hydroxy-N-methylacetamide

PubChem CID - 25713

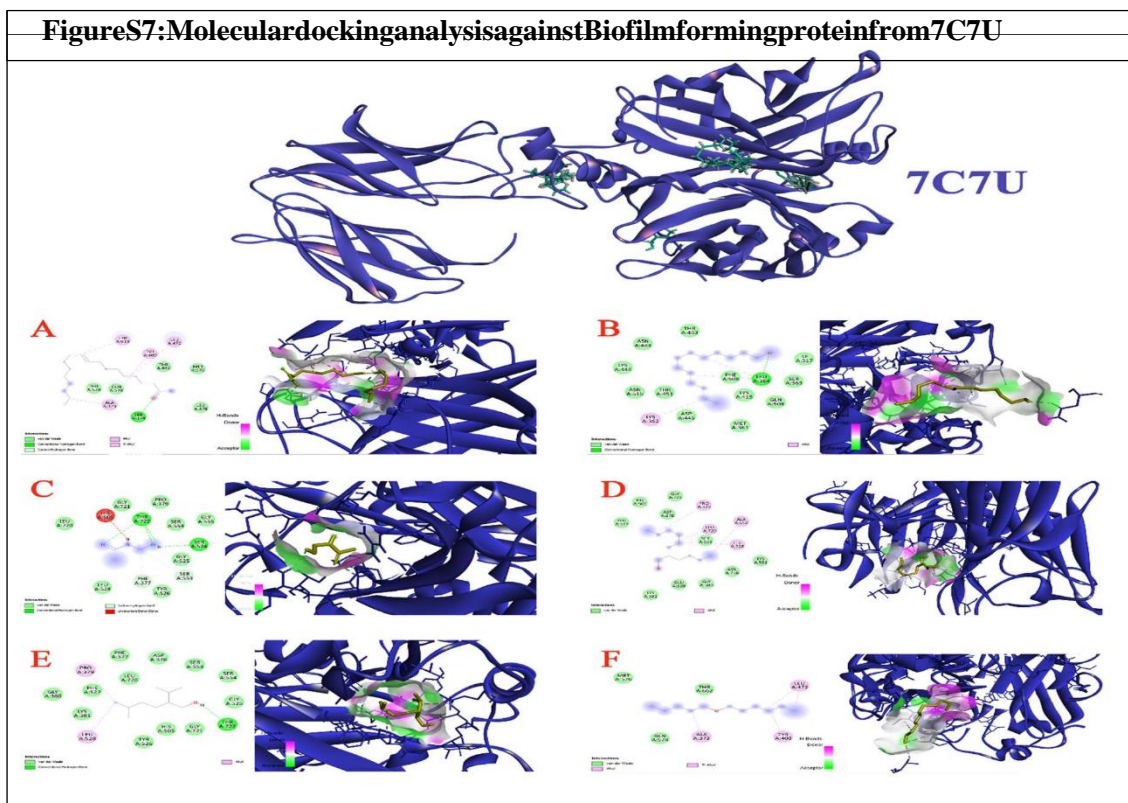
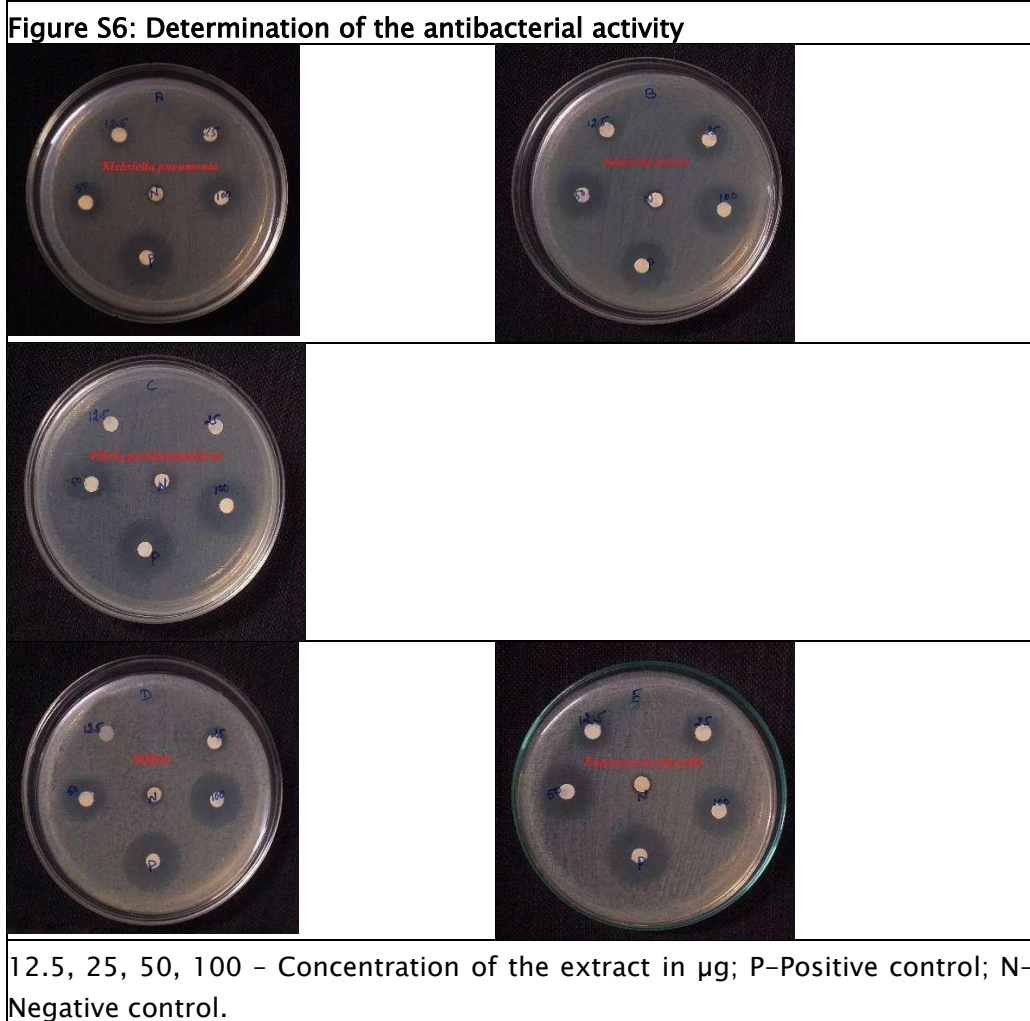


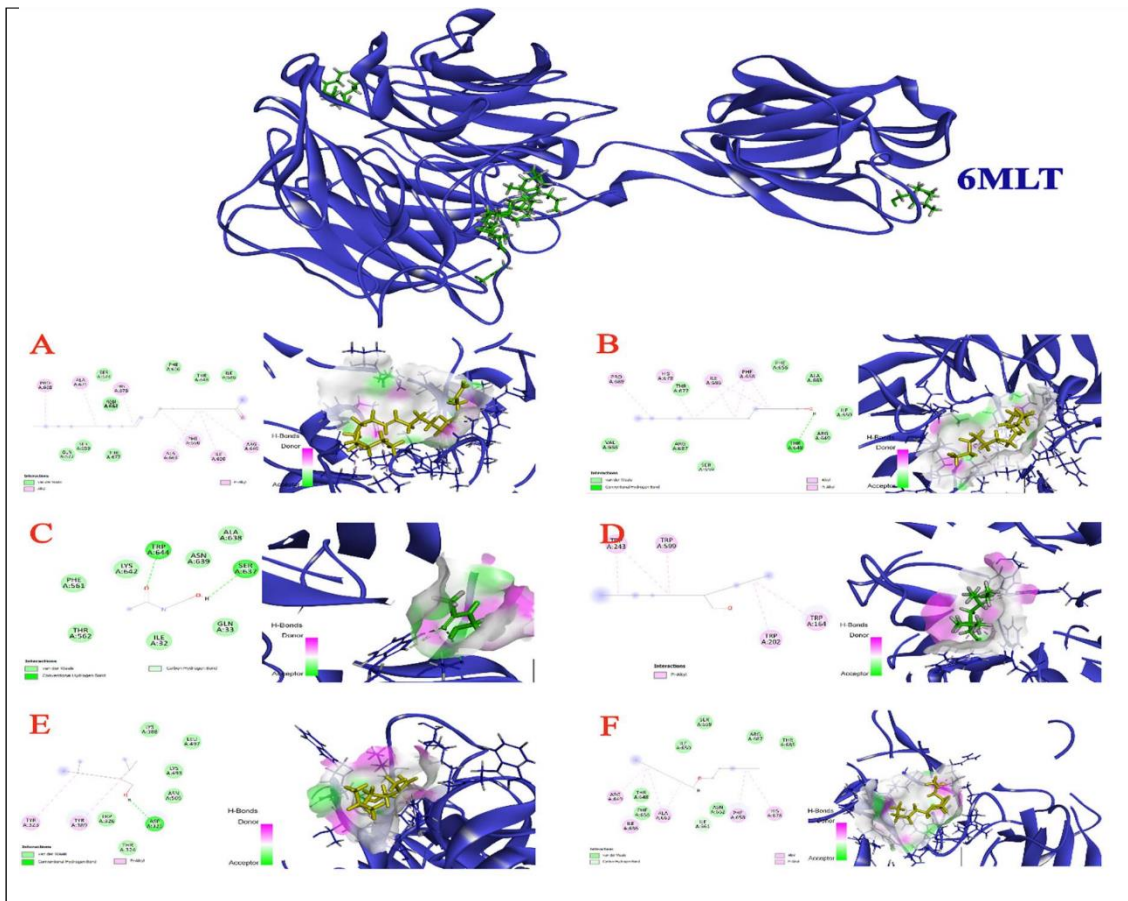
- Family A G protein-coupled receptor
- Enzyme
- Phosphatase
- Eraser
- Voltage-gated ion channel
- Kinase

Swiss Target Prediction



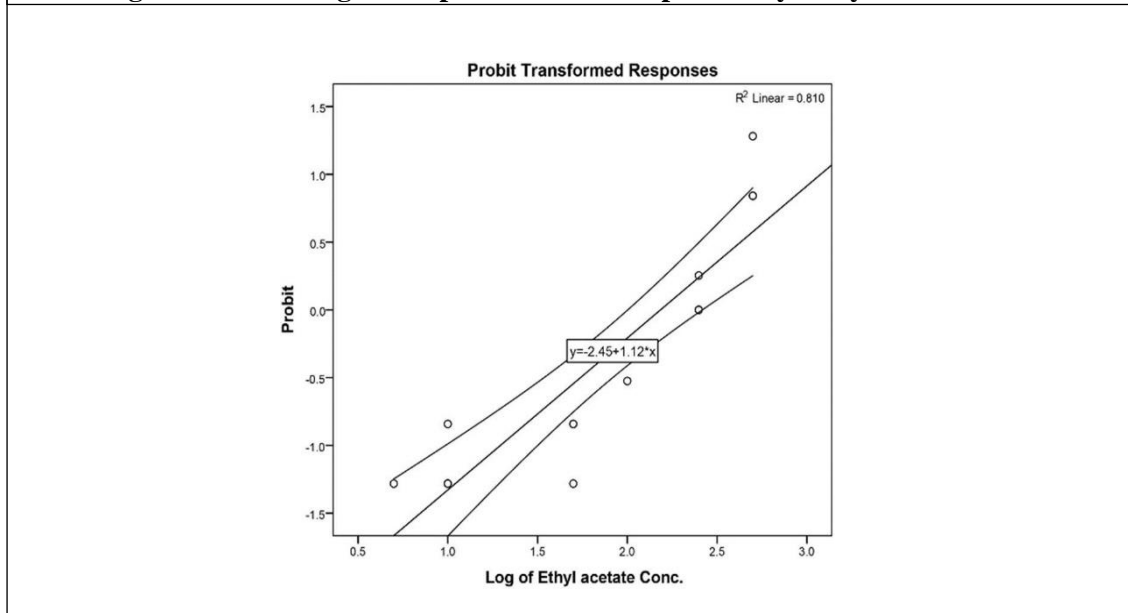
Physicochemical space for oral availability

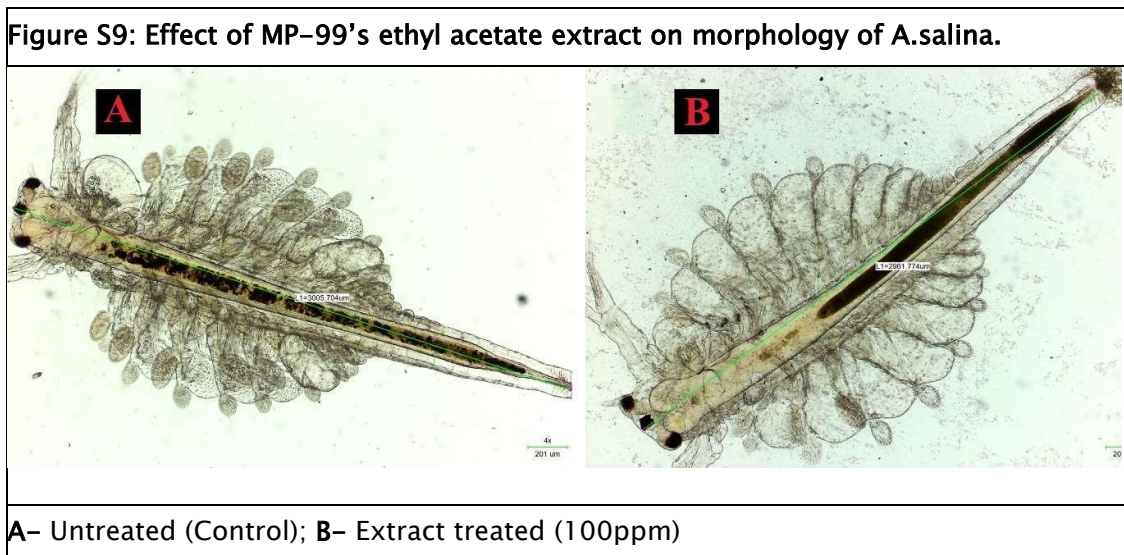




7C7U-Biofilmassociatedprotein(BSP);**6MLT**-BiofilmmatrixproteinBap1;
A-9octadecenamide;**B**-1Tridecanol;**C**-Nhydroxymethylacetamide;**D**-
 1octanol,**E**2butyl;

FigureS8:LinearregressionplotofBrineShrimpLethalityAssay-BSLA





REFERENCE:

- Bonhomme, S., Contreras-Martel, C., Dessen, A., & Macheboeuf, P. (2023). Architecture of a PKS-NRPS hybrid megaenzyme involved in the biosynthesis of the genotoxin colibactin. *Structure*. <https://doi.org/10.1016/j.str.2023.03.012>
- Cox, R. J. (2023). Curiouser and curiouser: progress in understanding the programming of iterative highly-reducing polyketide synthases. *Natural Product Reports*, 40(1), 9–27. <https://doi.org/10.1039/D2NP00007E>
- Chin, K. W., Michelle, T. H. L., Luang-In, V., & Ma, N. L. (2022). An overview of antibiotic and antibiotic resistance. *Environmental Advances*, 100331.
- Wibowo, J. T., Bayu, A., Aryati, W. D., Fernandes, C., Yanuar, A., Kijjoa, A., & Putra, M. Y. (2023). Secondary Metabolites from Marine-Derived Bacteria with Antibiotic and Antibiofilm Activities against Drug-Resistant Pathogens. *Marine Drugs*, 21(1), 50. <https://doi.org/10.3390/md21010050>
- Finglas, P. M., Wright, A. J., Wolfe, C. A., Hart, D. J., Wright, D. M., & Dainty, J. R. (2003). Is there more to folates than neural-tube defects?. *Proceedings of the Nutrition Society*, 62(3), 591–598. <https://doi.org/10.1079/PNS2003271>
- Stelmasiewicz, M., Świątek, Ł., Gibbons, S., & Ludwiczuk, A. (2023). Bioactive Compounds Produced by Endophytic Microorganisms Associated with Bryophytes—The “Bryendophytes”. *Molecules*, 28(7), 3246. <https://doi.org/10.3390/molecules28073246>
- Srinivasan, R., Kannappan, A., Shi, C., & Lin, X. (2021). Marine bacterial secondary metabolites: A treasure house for structurally unique and effective antimicrobial compounds. *Marine Drugs*, 19(10), 530. <https://doi.org/10.3390/md19100530>.
- Flemming, H. C., & Wuertz, S. (2019). Bacteria and archaea on Earth and their abundance in biofilms. *Nature Reviews Microbiology*, 17(4), 247–260. <https://doi.org/10.1038/s41579-019-0158-9>
- De Vos, W. M. (2015). Microbial biofilms and the human intestinal microbiome. *NPJ biofilms and microbiomes*, 1(1), 1–3. <https://doi.org/10.1038/npjbiofilms.2015.5>
- Qvortrup, K., Hultqvist, L. D., Nilsson, M., Jakobsen, T. H., Jansen, C. U., Uhd, J., ... & Tolker-Nielsen, T. (2019). Small molecule anti-biofilm agents developed on the basis of mechanistic understanding of biofilm formation. *Frontiers in chemistry*, 7, 742. <https://doi.org/10.3389/fchem.2019.00742>
- Flemming, H. C., Wingender, J. The biofilm matrix. *Nat Rev Microbiol* 8, 623–633 (2010).

<https://doi.org/10.1038/nrmicro2415>

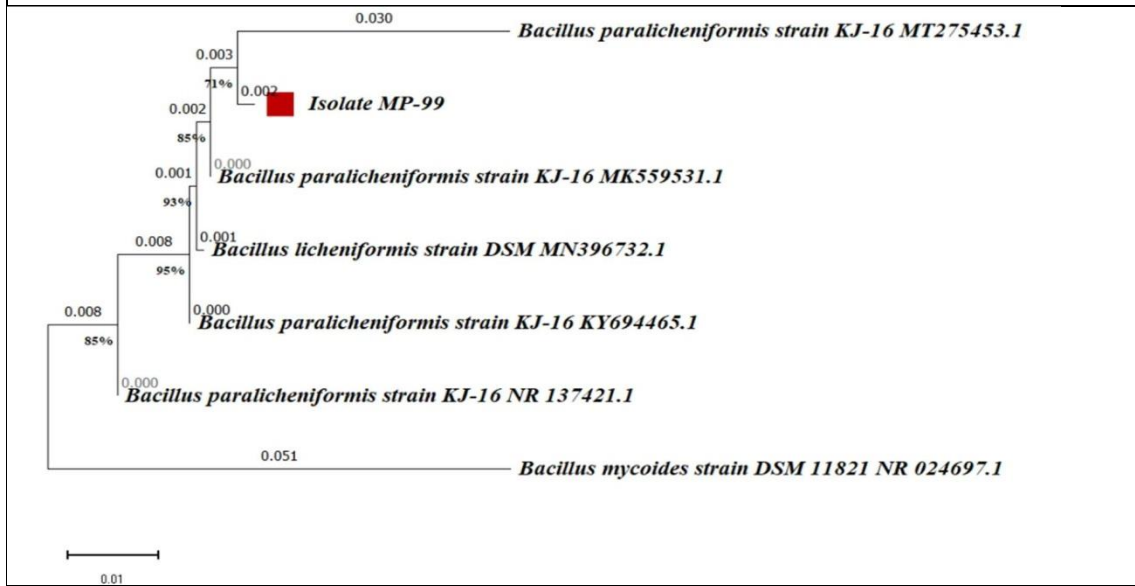
12. Branda, S. S., Vik, Å., Friedman, L., & Kolter, R. (2005). Biofilms: the matrix revisited. *Trends in microbiology*, 13(1), 20–26. <https://doi.org/10.1016/j.tim.2004.11.006>
13. Zhang, L., Liang, E., Cheng, Y., Mahmood, T., Ge, F., Zhou, K.,..... & Tan, Y. (2020). Is combined medication with natural medicine a promising therapy for bacterial biofilm infection?. *Biomedicine&pharmacotherapy*, 128, 110184 <https://doi.org/10.1016/j.biopha.2020.110184>
14. ZoBell, C. E. (1941). Studies on marine bacteria. I. The cultural requirements of heterotrophic aerobes.
15. Hagaggi, N. S. A., & Abdul-Raouf, U. M. (2022). Macroalga-associated bacterial endophyte bioactive secondary metabolites twinning: *Cystoseira myrica* and its associated *Catenococcus thiocycli* QCM as a model. *World Journal of Microbiology and Biotechnology*, 38(11), 205. <https://doi.org/10.1007/s11274-022-03394-2>
16. Kaewkla, O., & Franco, C. M. (2013). Rational approaches to improving the isolation of endophytic actinobacteria from Australian native trees. *Microbial Ecology*, 65, 384– 393. <https://doi.org/10.1007/s00248-012-0113-z>
17. Etmnani, F., Harighi, B., & Mozafari, A. A. (2022). Effect of volatile compounds produced by endophytic bacteria on virulence traits of grapevine crown gall pathogen, *Agrobacterium tumefaciens*. *Scientific Reports*, 12(1), 10510. <https://doi.org/10.1038/s41598-022-14864-w>
18. Al-Daghistani, H. I., Abu-Niaaj, L. F., Bustanji, Y., Al-Hamaideh, K. D., Al-Salamat, H., Nassar, M. N., & Al-Nuaimi, A. (2021). Antibacterial and cytotoxicity evaluation of *Arum hygrophilum* Bioss. *European Review for Medical and Pharmacological Sciences*, 25(23), 7306–7316.
19. Ibrahim, H., El-Zairy, E. M., Emam, E. A. M., & Saad, E. A. (2019). Combined antimicrobial finishing & dyeing properties of cotton, polyester fabrics and their blends with acid and disperse dyes. *egyptian Journal of Chemistry*, 62(5), 965–976. <https://doi.org/10.21608/EJCHEM.2018.6358.1535>
20. Le, T. H., Sivachidambaram, V., Yi, X., Li, X., & Zhou, Z. (2014). Quantification of polyketide synthase genes in tropical urban soils using real-time PCR. *Journal of microbiological methods*, 106, 135–142. <https://doi.org/10.1016/j.mimet.2014.08.010>
21. Metsä-Ketelä, M., Salo, V., Halo, L., Hautala, A., Hakala, J., Mäntsälä, P., & Ylihonko, K. (1999). An efficient approach for screening minimal PKS genes from *Streptomyces*. *FEMS Microbiology Letters*, 180(1), 1–6. <https://doi.org/10.1111/j.1574-6968.1999.tb08770.x>
22. Yuan, M., Yu, Y., Li, H. R., Dong, N., & Zhang, X. H. (2014). Phylogenetic diversity and biological activity of actinobacteria isolated from the Chukchi Shelf marine sediments in the Arctic Ocean. *Marine drugs*, 12(3), 1281–1297. <https://doi.org/10.3390/md12031281>
23. Ashrafian, B., & Hosseini-Abari, A. (2022). Investigation of bioactivity of unsaturated oligo-galacturonic acids produced from apple waste by *Alcaligenes faecalis* AGS3 and *Paenibacillus polymyxa* S4 Pectinases. *Scientific Reports*, 12(1), 15830. <https://doi.org/10.1038/s41598-022-20011-2>
24. Yadav, P., Korpole, S., Prasad, G. S., Sahni, G., Maharjan, J., Sreerama, L., & Bhattarai, T. (2018). Morphological, enzymatic screening, and phylogenetic analysis of thermophilic bacilli isolated from five hot springs of Myagdi, Nepal. *Journal of Applied Biology and Biotechnology*, 6(3), 1–8. <https://doi.org/10.7324/JABB.2018.60301>
25. Verma, A. M. B. I. K. A., Gupta, M. O. N. I. K. A., & Shirkot, P. O. O. N. A. M. (2014). Isolation and characterization of thermophilic bacteria in natural hot water springs of Himachal Pradesh (India). *The Bioscan*, 9(3), 947–952.

26. Pugazhendi, A., Abbad Wazin, H., Qari, H., Basahi, J. M. A. B., Godon, J. J., & Dhavamani, J. (2017). Biodegradation of low and high molecular weight hydrocarbons in petroleum refinery wastewater by a thermophilic bacterial consortium. *Environmental technology*, 38(19), 2381–2391. <https://doi.org/10.1080/09593330.2016.1262460>
27. Carvalho, M., Albano, H., & Teixeira, P. (2018). In vitro antimicrobial activities of various essential oils against pathogenic and spoilage microorganisms. *Journal of food quality and hazards control*, 5(2), 41–48. <https://doi.org/10.29252/jfqhc.5.2.3>
28. Requena, R., Vargas, M., & Chiralt, A. (2019). Study of the potential synergistic antibacterial activity of essential oil components using the thiazolyl blue tetrazolium bromide (MTT) assay. *Lwt*, 101, 183–190. <https://doi.org/10.1016/j.lwt.2018.10.093>
29. Sarker, S. D., Nahar, L., & Kumarasamy, Y. (2007). Microtitre plate-based antibacterial assay incorporating resazurin as an indicator of cell growth, and its application in the in vitro antibacterial screening of phytochemicals. *Methods*, 42(4), 321–324. <https://doi.org/10.1016/j.ymeth.2007.01.006>
30. Ye, H., Shen, S., Xu, J., Lin, S., Yuan, Y., & Jones, G. S. (2013). Synergistic interactions of cinnamaldehyde in combination with carvacrol against food-borne bacteria. *Food Control*, 34(2), 619–623. <https://doi.org/10.1016/j.foodcont.2013.05.032>
31. Liu, S., She, P., Li, Z., Li, Y., Li, L., Yang, Y., ... & Wu, Y. (2023). Antibacterial and antibiofilm efficacy of repurposing drug hexestrol against methicillin-resistant *Staphylococcus aureus*. *International Journal of Medical Microbiology*, 313(2), 151578. <https://doi.org/10.1016/j.ijmm.2023.151578>
32. Thayumanavan, G., Jeyabalan, S., Fuloria, S., Sekar, M., Ravi, M., Selvaraj, L. K., ... & Fuloria, N. K. (2022). Silibinin and Naringenin against Bisphenol A-Induced neurotoxicity in zebrafish model—Potential flavonoid molecules for new drug design, development, and therapy for neurological disorders. *Molecules*, 27(8), 2572. <https://doi.org/10.3390/molecules27082572>
33. Meyer, B. N., Ferrigni, N. R., Putnam, J. E., Jacobsen, L. B., Nichols, D. E. J., & McLaughlin, J. L. (1982). Brine shrimp: a convenient general bioassay for active plant constituents. *Planta medica*, 45(05), 31–34. <https://doi.org/10.1055/s-2007-971236>
34. Olajide, A. M., Chen, S., & LaPointe, G. (2021). Markers to rapidly distinguish *Bacillus paralicheniformis* from the very close relative, *Bacillus licheniformis*. *Frontiers in Microbiology*, 11, 596828. <https://doi.org/10.3389/fmicb.2020.596828>
35. Li, S. N., Zhang, C., Li, F., Ren, N. Q., & Ho, S. H. (2023). Recent advances of algae–bacteria consortia in aquatic remediation. *Critical Reviews in Environmental Science and Technology*, 53(3), 315–339. <https://doi.org/10.1080/10643389.2022.2052704>
36. Tanabe, Y., Yamaguchi, H., Yoshida, M., Kai, A., & Okazaki, Y. (2023). Characterization of a bloom-associated alphaproteobacterial lineage, 'CandidatusPhycosocius': insights into freshwater algal–bacterial interactions. *ISME communications*, 3(1), 20. <https://doi.org/10.1038/s43705-023-00228-6>
37. Pushpakumara, B. U., Tandon, K., Willis, A., & Verbruggen, H. (2023). The bacterial microbiome of the coral skeleton algal symbiont *Ostreobium* shows preferential associations and signatures of phyllosymbiosis. *Microbial Ecology*, 1–15. <https://doi.org/10.1007/s00248-023-02209-7>
38. Santos, O. C., Pontes, P. V., Santos, J. F., Muricy, G., Giambiagi-deMarval, M., & Laport, M. S. (2010). Isolation, characterization and phylogeny of sponge-associated bacteria with antimicrobial activities from Brazil. *Research in Microbiology*, 161(7), 604–612. <https://doi.org/10.1016/j.resmic.2010.05.013>
39. Thawabteh, A. M., Swaileh, Z., Ammar, M., Jaghama, W., Yousef, M., Karaman, R., ... & Scrano,

- L. (2023). Antifungal and antibacterial activities of isolated marine compounds. *Toxins*, 15(2), 93. <https://doi.org/10.3390/toxins15020093>
40. Martins, A., Vieira, H., Gaspar, H., & Santos, S. (2014). Marketed marine natural products in the pharmaceutical and cosmeceutical industries: Tips for success. *Marine drugs*, 12(2), 1066–1101. <https://doi.org/10.3390/md12021066>
41. Tran, C., Cock, I. E., Chen, X., & Feng, Y. (2022). Antimicrobial *Bacillus*: metabolites and their mode of action. *Antibiotics*, 11(1), 88. <https://doi.org/10.3390/antibiotics11010088>
42. Dimkić, I., Janakiev, T., Petrović, M., Degrassi, G., & Fira, D. (2022). Plant-associated *Bacillus* and *Pseudomonas* antimicrobial activities in plant disease suppression via biological control mechanisms—A review. *Physiological and Molecular Plant Pathology*, 117, 101754. <https://doi.org/10.1016/j.pmpp.2021.101754>
43. Raaijmakers, J. M., De Bruijn, I., Nybroe, O., & Ongena, M. (2010). Natural functions of lipopeptides from *Bacillus* and *Pseudomonas*: more than surfactants and antibiotics. *FEMS microbiology reviews*, 34(6), 1037–1062. <https://doi.org/10.1111/j.1574-6976.2010.00221.x>
44. Komaki, H., Sakurai, K., Hosoyama, A., Kimura, A., Igarashi, Y., & Tamura, T. (2018). Diversity of nonribosomal peptide synthetase and polyketide synthase gene clusters among taxonomically close *Streptomyces* strains. *Scientific reports*, 8(1), 6888. <https://doi.org/10.1038/s41598-018-24921-y>
45. Komaki, H., Sakurai, K., Hosoyama, A., Kimura, A., Trujillo, M. E., Igarashi, Y., & Tamura, T. (2020). Diversity of PKS and NRPS gene clusters between *Streptomyces abyssomicinicus* sp. nov. and its taxonomic neighbor. *The Journal of Antibiotics*, 73(3), 141–151. <https://doi.org/10.1038/s41429-019-0261-1>
46. Valenzuela Ruiz, V., Gándara-Ledezma, A., Villarreal-Delgado, M. F., Villa-Rodríguez, E. D., Parra-Cota, F. I., Santoyo, G., & de los Santos-Villalobos, S. (2024). Regulation, Biosynthesis, and Extraction of *Bacillus*-Derived Lipopeptides and Its Implications in Biological Control of Phytopathogens. *Stresses*, 4(1), 107–132. <https://doi.org/10.3390/stresses4010007>
47. Chen, M., Wang, J., Liu, B., Zhu, Y., Xiao, R., Yang, W., ... & Chen, Z. (2020). Biocontrol of tomato bacterial wilt by the new strain *Bacillus velezensis* FJAT-46737 and its lipopeptides. *BMC microbiology*, 20(1), 1–12. <https://doi.org/10.1186/s12866-020-01851-2>
48. Johnson, B. A., Anker, H., & Meleney, F. L. (1945). Bacitracin: a new antibiotic produced by a member of the *B. subtilis* group. *Science*, 102(2650), 376–377. <https://doi.org/10.1126/science.102.2650.376>
49. Choi, Y. H., Cho, S. S., Simkhada, J. R., Rahman, M. S., Choi, Y. S., Kim, C. S., & Yoo, J. C. (2017). A novel multifunctional peptide oligomer of bacitracin with possible bioindustrial and therapeutic applications from a Korean food-source *Bacillus* strain. *PLoS One*, 12(5), e0176971. <https://doi.org/10.1371/journal.pone.0176971>
50. Ahire, J.J., Kashikar, M.S., Lakshmi, S.G. et al. Identification and characterization of antimicrobial peptide produced by indigenously isolated *Bacillus paralicheniformis* UBBLi30 strain. *3 Biotech* 10, 112 (2020). <https://doi.org/10.1007/s13205-020-2109-6>
51. Iqbal, S., Qasim, M., Rahman, H., Khan, N., Paracha, R. Z., Bhatti, M. F., ... & Janjua, H. A. (2023). Genome mining, antimicrobial and plant growth-promoting potentials of halotolerant *Bacillus paralicheniformis* ES-1 isolated from salt mine. *Molecular Genetics and Genomics*, 298(1), 79–93. <https://doi.org/10.1007/s00438-022-01964-5>
52. Choyam, S., Jain, P. M., & Kammar, R. (2021). Characterization of a potent new-generation antimicrobial peptide of *Bacillus*. *Frontiers in Microbiology*, 12, 710741. <https://doi.org/10.3389/fmicb.2021.710741>

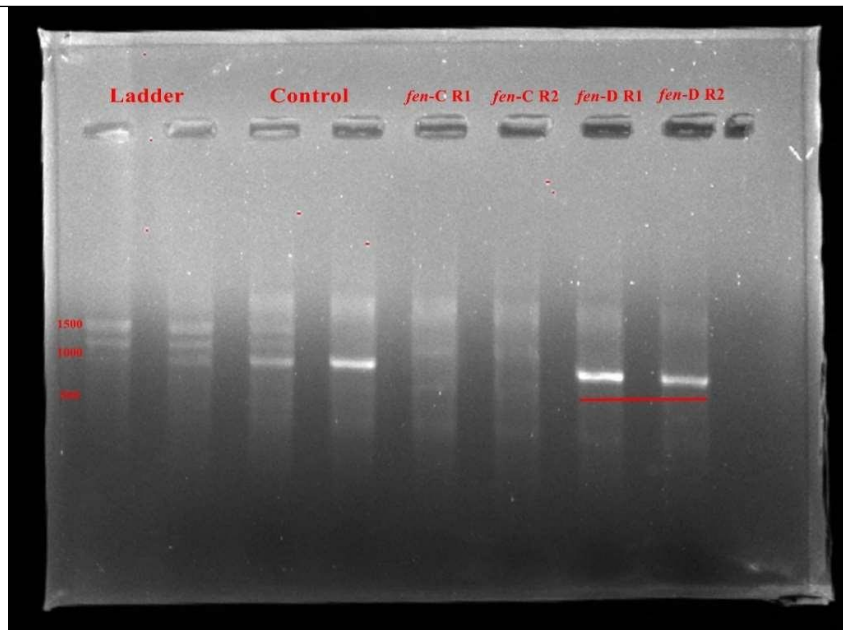
53. Kaushik A, Kest H, Sood M, Steussy BW, Thieman C, Gupta S. Biofilm Producing Methicillin-Resistant *Staphylococcus aureus* (MRSA) Infections in Humans: Clinical Implications and Management. *Pathogens*. 2024; 13(1):76. <https://doi.org/10.3390/pathogens13010076>
54. Meparambu Prabhakaran, D., Ramamurthy, T., & Thomas, S. (2020). Genetic and virulence characterisation of *Vibrio parahaemolyticus* isolated from Indian coast. *BMC microbiology*, 20(1), 1–14. <https://doi.org/10.1186/s12866-020-01746-2>
55. Zhang, Y., Qiu, Y., Xue, X., Zhang, M., Sun, J., Li, X., ... & Zhou, D. (2021). Transcriptional regulation of the virulence genes and the biofilm formation associated operons in *Vibrio parahaemolyticus*. *Gut Pathogens*, 13, 1–10. <https://doi.org/10.1186/s13099-021-00410-y>
56. Wang, Q., Wang, P., Liu, P., & Ou, J. (2022). Comparative Transcriptome Analysis Reveals Regulatory Factors Involved in *Vibrio Parahaemolyticus* Biofilm Formation. *Frontiers in Cellular and Infection Microbiology*, 12, 917131. <https://doi.org/10.3389/fcimb.2022.917131>
57. Qian, H., Li, W., Guo, L., Tan, L., Liu, H., Wang, J., ... & Zhao, Y. (2020). Stress response of *Vibrio parahaemolyticus* and *Listeria monocytogenes* biofilms to different modified atmospheres. *Frontiers in Microbiology*, 11, 23. <https://doi.org/10.3389/fmicb.2020.00023>
58. Nithya, C., Begum, M., & Pandian, S. (2010). Marine bacterial isolates inhibit biofilm formation and disrupt mature biofilms of *Pseudomonas aeruginosa* PAO1. *Applied Microbiology and Biotechnology*, 88, 341–358. <https://doi.org/10.1007/s00253-010-2777-y>.
59. Khidre, R.E., Sabry, E., El-Sayed, A.F. et al. Design, one-pot synthesis, in silico ADMET prediction and molecular docking of novel triazolyl thiadiazine and thiazole derivatives with evaluation of antimicrobial, antioxidant and antibiofilm inhibition activity. *J IRAN CHEM SOC* 20, 2923–2947 (2023). <https://doi.org/10.1007/s13738-023-02889-5>.
60. Moniruzzaman, M., Jinnah, M. M., Islam, S., Biswas, J., Pramanik, M. J., Uddin, M. S.,... & Zaman, S. (2022). Biological activity of *Cucurbita maxima* and *Momordica charantia* seed extracts against the biofilm-associated protein of *Staphylococcus aureus*: An in vitro and in silico studies. *Informatics in Medicine Unlocked*, 33, <https://doi.org/10.1016/j.imu.2022.101089>
61. Clarkson, C., Maharaj, V. J., Crouch, N. R., Grace, O. M., Pillay, P., Matsabisa, M. G.,...& Folb, P. I. (2004). In vitro antiplasmodial activity of medicinal plants native to or naturalised in South Africa. *Journal of ethnopharmacology*, 92(2–3), 177–191. <https://doi.org/10.1016/j.jep.2004.02.011> .

Figure 1: Neighbor-joining tree based on 16S rRNA gene sequence.



The Phylogenetic showing the relationship between isolate MP-99 and related species. Bootstrap values (based on 1000 replications) are shown at branch points. Bar, 0.01 substitutions per nucleotide position.

Figure:2Gel resolution of Fengycin based amplicons



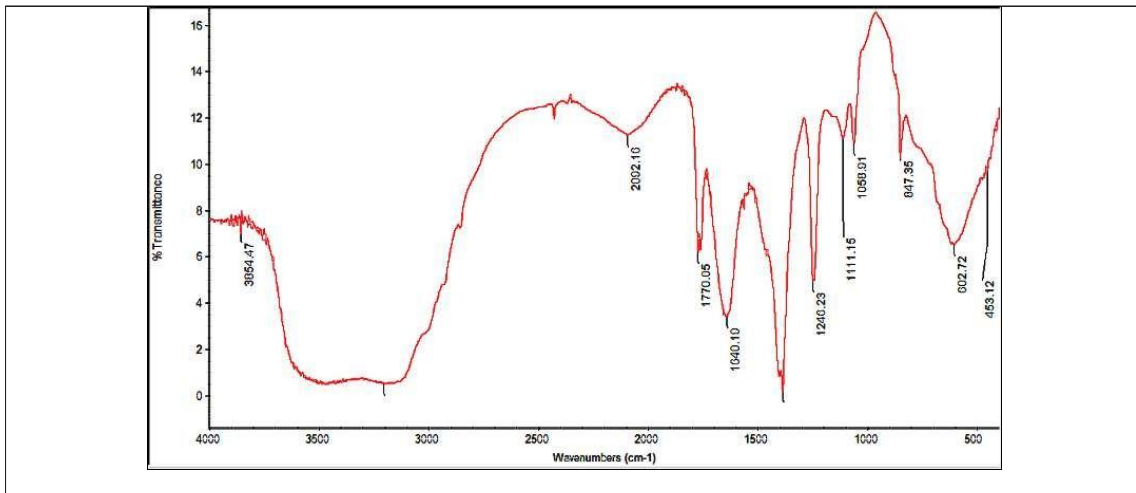


Figure:3FT-IRpeaksofIsolateMP-99'sEthylAcetateExtract

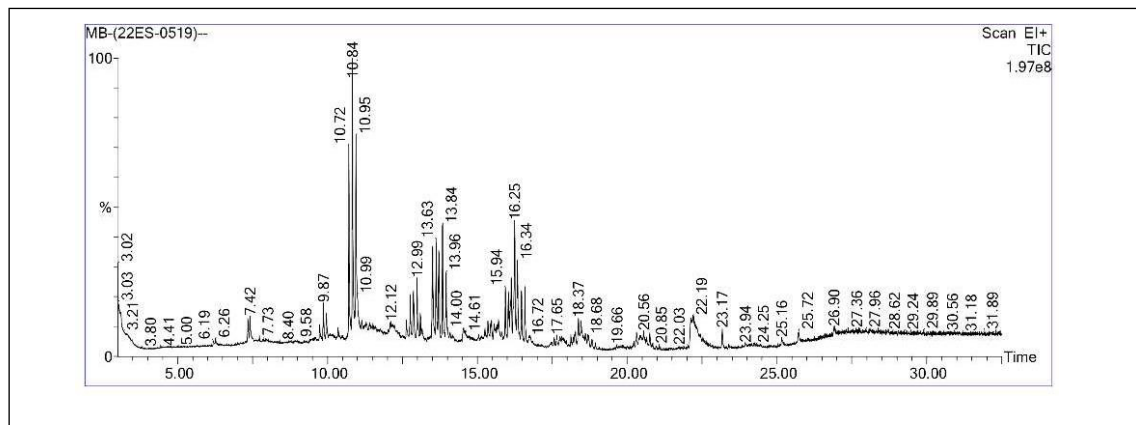


Figure:4GC-MSAnalysisofIsolateMP-99'sEthylAcetateExtract

Figure5:AntibiofilmactivityagainsttheDrugresistantBiofilmformingbacteria

